SECURITY CLASSIFICATION OF THIS PAGE

REPORT DOCUMENTATION PAGE

Form Approved
OMB No. 0704-0188

AD-A209 866

1b. RESTRICTIVE MARKINGS

3. DISTRIBUTION/AVAILABILITY OF REPORT
Approved for public release; distribution unlimited.

4. PERFORMING ORGANIZATION REPORT NUMBER(S)

5. MONITORING ORGANIZATION REPORT NUMBER(S)
AFOSR-TR- 89-0884

6a. NAME OF PERFORMING ORGANIZATION
Michigan Technological University
Department of Metallurgical Engineering

6b. OFFICE SYMBOL (If applicable)

7a. NAME OF MONITORING ORGANIZATION
AFOSR

6c. ADDRESS (City, State, and ZIP Code)

7b. ADDRESS (City, State, and ZIP Code)
BLDG 410
BAFB DC 20332-6448

8a. NAME OF FUNDING/SPONSORING ORGANIZATION
AFOSR

8b. OFFICE SYMBOL (If applicable)

9. PROCUREMENT INSTRUMENT IDENTIFICATION NUMBER
AFOSR-78-3728

8c. ADDRESS (City, State, and ZIP Code)
BLDG 410
BAFB DC 20332-6448

10. SOURCE OF FUNDING NUMBERS

PROGRAM ELEMENT NO.	PROJECT NO.	TASK NO.	WORK UNIT ACCESSION NO.
61102F	2306	A1	

11. TITLE (Include Security Classification)
FUNDAMENTAL STUDIES OF B PHASE DECOMPOSITION MODES IN TITANIUM ALLOYS

12. PERSONAL AUTHOR(S)
H.I Aaronson,/G.K. Scarr/M.R. Plichta/ J.P. Moore

13a. TYPE OF REPORT	13b. TIME COVERED	14. DATE OF REPORT (Year, Month, Day)	15. PAGE COUNT
Final	FROM 10/1/78 TO 9/30/79	August 17, 1979	32

16. SUPPLEMENTARY NOTATION

17. COSATI CODES			18. SUBJECT TERMS (Continue on reverse if necessary and identify by block number)
FIELD	GROUP	SUB-GROUP	

19. ABSTRACT (Continue on reverse if necessary and identify by block number)

20. DISTRIBUTION/AVAILABILITY OF ABSTRACT
☒ UNCLASSIFIED/UNLIMITED ☐ SAME AS RPT. ☐ DTIC USERS

21. ABSTRACT SECURITY CLASSIFICATION
Unclassified

22a. NAME OF RESPONSIBLE INDIVIDUAL

22b. TELEPHONE (Include Area Code)
767-4984

22c. OFFICE SYMBOL
NE

DD Form 1473, JUN 86 Previous editions are obsolete. SECURITY CLASSIFICATION OF THIS PAGE

Final ~~Interim~~ Technical Report

from

Department of Metallurgical Engineering
Michigan Technological University

to

Air Force Office of Scientific Research
Room C211
Bolling Air Force Base
Washington, DC 20332

on

Fundamental Studies of β Phase Decomposition Modes in Titanium Alloys

by

H. I. Aaronson, Principal Investigator
G. K. Scarr, Postdoctoral Research Associate
M. R. Plichta, Graduate Research Assistant
J. P. Moore, Graduate Research Assistant

for the period

1 October 1978 - 30 September 1979

August 17, 1979

Fundamental Studies of β Phase Decomposition Modes in Titanium Alloys

H. I. Aaronson, G. K. Scarr, M. R. Plichta and J. P. Moore

Abstract

A technique has been developed for preparing thin foils of Ti-X specimens containing α, β and intermetallic compound based upon ion milling performed in a cold stage without any intermediate electrothinning. Application of this technique to a Ti-6 W/O Cr alloy reacted at 625°C yielded the following orientation relationships among the three phases: $(0001)_\alpha // (110)_\beta // (111)_{TiCr_2}$, $[11\bar{2}0]_\alpha // [1\bar{1}\bar{1}]_\beta // [1\bar{2}1]_{TiCr_2}$. This result is in accord with a prediction of our theory of precipitation at interphase boundaries. A selected area electron channeling pattern study has been made of orientation relationships developed during the massive transformation b.c.c. $\beta \rightarrow$ h.c.p. ζ_m in a Ag-26 A/O Al alloy. All ζ_m crystals studied precipitated at β grain faces or edges. Of the 47 ζ_m crystals analyzed, 46 had exactly or almost a Burgers orientation relationship with respect to at least one β grain; many of the other orientation relationships observed were rational and some of these were shown by an O-lattice analysis to correspond to a partially coherent interphase boundary. But nearly all $\beta:\zeta_m$ interfaces were clearly faceted, indicating that partially coherent boundaries, and hence low energy orientation relationships, tended to occur with all β grains with which the ζ_m nucleus was in contact, in agreement with predictions based upon Gibbsian nucleation theory. Refinement of the models used for critical nuclei formed during the $\beta \rightarrow \alpha_m$ reaction in Ti-Ag and Ti-Au alloys has shown that acceptable interfacial energies for the edges of pillbox-shaped nuclei can still be obtained even when one face of the pillbox has a disordered structure and thus takes the shape of a spherical cap. Consistency is thus achieved with the Ag-Al results in situations where disordered $\beta:\zeta_m$ boundaries do develop. The f.c.c. $\alpha \rightarrow$ h.c.p. α_2 massive

transformation in a Au-30 A/O Cd alloy has been shown to yield plate-shaped massive α_2 (in agreement with our views but in sharp disagreement with the current "conventional wisdom"), to exhibit acceptable transformation kinetics, to permit extensive retention of untransformed α and to have not too high a density of stacking faults in either phase. This transformation has accordingly been selected as our model of an f.c.c.→h.c.p. massive transformation and is expected to provide a definitive test of the alleged non-role of crystallography in massive transformations.

I. Introduction

This program consists of fundamental studies of the mechanisms of the massive and bainite reactions in Ti-X eutectoid systems, supplemented by an investigation of the massive transformation in a Ag-26 A/O Al alloy serving as a crystallographic "stand-in" for the bcc→hcp massive transformation in titanium alloys and by a study of the fcc→hcp massive transformation modeled in Au-Cd alloys in order to follow up and further test the conclusions about the mechanism of massive transformations in general drawn from the initial studies of this reaction in Ti-X alloys.

For the purposes of this investigation, the generalized microstructural definition of bainite is employed. On this definition (1), bainite is a non-lamellar product of eutectoid decomposition wherein the two low temperature phases precipitate sequentially, rather than synchronously, and do so in a manner which results in the development of non-lamellar particles of the minority phase amongst crystals of the majority phase formed in diverse morphologies. The majority phase, here proeutectoid α, need not have a plate or needle morphology, though in Ti-X alloys it often does.

The massive transformation takes place by the conversion of the matrix to the product phase without a change in composition by means of a diffusional nucleation and growth mechanism. Diffusional jumps across the matrix:massive interphase boundary is the basic atomic process involved in this transformation. Since no long-range diffusion is required, and especially no volume diffusion, growth rates achieved during a massive transformation are often five or more orders of magnitude higher than those accompanying precipitate growth by volume diffusion-control.

II. The Bainite Reaction in Ti-X Alloys
(Dr. G. K. Scarr, Postdoctoral Research Associate)

Success has finally been achieved in obtaining electron diffraction data from adjacent crystals of α, β and intermetallic compound in a titanium bainite structure, and thus in determining the orientation relationships amongst these three phases. This result was secured in a Ti-6% Cr alloy, and efforts are being pressed to repeat the initial success at other temperature in this alloy and in many other Ti-X alloy systems.

In our previous annual technical report we indicated the advantages of ion beam milling TEM foils which had already been perforated by electro-thinning to displace the electron transparent region to regions of the specimen containing all three phases. Although this approach proved very useful the difficulty remained that the different phases were still of quite unequal thickness. The $TiCr_2$, in particular, which remained thickest of all, gave barely adequate diffraction patterns when the foil was kept flat in the microscope. The increase in the thickness of foil which the electron beam had to traverse when the foil was tilted, however, prevented any diffraction pattern from being secured at many important orientations of the foil.

The next approach taken was that of producing a thin foil by ion milling alone after mechanical grinding had been completed. This procedure had been previously avoided because ion milling is inherently inferior to electro-polishing in that it cannot produce a very uniform specimen profile around the edges of the hole. Instead of obtaining a thin region which can be followed continuously from one region of the foil to another the profile of an ion milled specimen is very irregular and pock-marked so that it is difficult to obtain good low magnification images. These are important for connecting the TEM to the optical microstructure. Also, ion milling specimens

which had been previously electropolished were found to cause a marked reduction in total thin area, even at the lowest angles of incidence at which milling could be achieved, without reducing the thickness differential between phases.

However, ion milling from mechanically ground discs proved much more satisfactory than was originally anticipated. The total thin area was found to be larger than that obtained from other methods. The appearance of multiple perforations and the serrated and re-entrant nature of the main hole more than compensates for the limited amount of thin area per hole. Further, the presence of a number of holes appears to increase the probability that one of them will appear in a region of the foil containing all three phases.

Three other benefits have arisen from direct ion milling. First, and most importantly, the erosion rate for each phase is very similar, if not equal. In retrospect it seems obvious that ion-milling did not appear beneficial when applied to the electropolished specimens because it was attacking each phase equally and could not eradicate the thickness differential produced by the electropolishing. A second advantage is that the small size of each thin region, though diadavantageous per se, results in much better physical support being provided to each thin area by the surrounding thicker region. This factor, and possibly also the absence of an impinging jet of electrolyte during thinning, results in less foil bending. Thus areas which are not immediately adjacent can be compared crystallographically without large errors due to foil bending. Sharper Kikuchi lines are also obtained, a matter of much importance in the determination of orientation relationships.

Finally, the serrated "non-Burgers α" which appears in Burgers α at α:β interfaces (2,3) is not observed in specimens produced by direct ion

milling. It appears that ion milling may actually be destablizing and destroying the non-Burgers α which is otherwise of quite frequent occurrence in Ti-Cr specimens. The possibility that foil heating during ion milling may be responsible in some way has been excluded by doing the milling in a cold stage at -25°C; the same result was obtained. We plan to discuss this interesting development further with Prof. J. C. Williams at Carnegie-Mellon University during the Fall. For present purposes, however, the disappearance of non-Burgers α is a most useful side effect of the direct ion milling technique since it much facilitates determination of the orientation of the α phase and also frees the α:β interface from an encumbrance which can prevent observations on the nucleation sites of compound particles.

Employing a directly ion milled foil, the following orientation relationships have been determined among the three phases involved in the bainite reaction in a Ti-6 W/O Cr alloy:

$$(0001)_{\alpha}//(110)_{\beta}//(111)_{TiCr_2}$$

$$[11\bar{2}0]_{\alpha}//[1\bar{1}1]_{\beta}//[1\bar{2}1]_{TiCr_2}$$

The relationship between α and β is the Burgers (4) orientation relationship; this corresponds to good matching between these two phases. Although the $TiCr_2$ phase is a complex, ordered variant of the f.c.c. structure, the relationship between α and $TiCr_2$ is the standard low energy f.c.c.:h.c.p. orientation relationship of best matching. The level of interface matching between β and $TiCr_2$ made possible by the orientation relationship determined between these two phases will be investigated shortly by means of the computer program developed during the massive transformation portion of this investigation.

Because of our impending move to Carnegie-Mellon University, with the inevitable attendant suspension of heat treatment until our equipment can be installed at CMU and restored to full operation, the immediate

focus of this investigation has shifted to an extensive program of specimen encapsulation and heat treatment. Many different Ti-X alloys are presently being heat treated in order to have at hand a large array of specimens for processing into thin foils for TEM studies, to be initiated soon after we reach Carnegie-Mellon University.

In the course of these heat treatments, though, some preliminary TEM studies have been made. It has been observed that the nucleation and/or the growth of intermetallic compound crystals appears different in Ti-Bi and Ti-Pb alloys than in the other Ti-X alloys examined. Evidently this difference derives directly from the "bulkier" proeutectoid α morphology produced in these two systems. We hypothesize that this difference arises from a difference in interfacial structure, at least in the form of an appreciably higher density of growth ledges. Hence Ti-Bi and Ti-Pb appear to be good candidates for early studies of β:α interfacial structure.

III. The Massive Transformation

A. Crystallography of the $\beta \rightarrow \zeta_m$ Transformation in Ag-26 A/O Al

(M. R. Plichta, Graduate Student)

The crystallography of this massive transformation, of a b.c.c. matrix to an h.c.p. product phase, is being investigated as a "stand-in" for the crystallographically equivalent $\beta \rightarrow \alpha_m$ transformations in Ti-Ag, Ti-Au and Ti-Si. The high M_s temperatures in these three Ti-X systems, the only ones of eutectoid type known to undergo β decomposition by a massive transformation, prevent retention of the β matrix and thus determination of the crystallographic relationships between β and α_m.

At the time of our previous report the experimental difficulties encountered in attempting to obtain electron transparent regions at faceted β:ζ_m interfaces were thought to have been solved. Although the cryogenic stage purchased for use in conjunction with this Department's ion miller

(which we have termed the "miller chiller") proved successful in preventing precipitation of ω phase, two additional problems developed:

(1) Lengthy milling, required to effect the necessary displacement of the electron transparent areas to $\beta:\zeta_m$ interfaces, causes considerable surface damage to foils, to the point where they become unusable for weak-beam, dark-field analysis (5).

(2) When $\beta:\zeta_m$ facets finally were obtained in thin areas, they were invariably perpendicular to the foil surfaces. The amount of foil tilting required to permit examination of the interfacial structure caused the effective thickness of the foil to increase to the point where the weak-beam, dark-field technique again could not be utilized.

The interfacial structure portion of this investigation has accordingly been terminated. Attention has been re-directed toward a less direct, but still very useful attack upon the problem of ascertaining whether or not specific, low energy orientation relationships obtain between the matrix and massive phases. Using the electron channeling capability of this Department's new JEM-100CX, orientation relationships have been determined between 47 ζ_m crystals, all nucleated at β grain faces or edges, and the β grains forming these boundaries. The following results have been obtained from these determinations:

(1) 46 of the 47 ζ_m crystals analyzed had exactly or almost exactly a Burgers orientation relationship (5) with respect to at least one of the parent β grains:

$$(0001)_{\zeta_m} // (110)_\beta$$

$$[11\bar{2}0]_{\zeta_m} // [1\bar{1}1]_\beta$$

The discrepant ζ_m crystal was very large and likely flrmed at a grain boundary below the specimen surface.

(2) Often, but not always, the ζ_m crystals grew preferentially into the β matrix grain with respect to which they were not Burgers oriented. An equivalent result has been previously reported for the β(b.c.c.)$\rightarrow\alpha_m$(f.c.c.) Ag-Zn transformation by Ayres and Joy (6).

(3) Similarly shaped ζ_m nucleated at a β grain boundary with an approximately constant boundary orientation had the same spatial orientation to within $\pm$ 1°.

(4) Primary ζ_m sideplates were observed at a small-angle twist grain boundary (Figure 1). In precipitation reactions, small-angle grain boundaries give rise to primary sideplates when the matrix has a f.c.c. structure and sometime also when it has a b.c.c. structure (7).

(5) Examination of the orientation relationships between ζ_m crystals and the β grains with respect to which they were not Burgers related indicated that in five cases of nucleation at β grain faces no reasonably low indices planes or directions were parallel in the two phases. In the remaining five cases of grain face nucleation, such pairs of parallel planes and directions were observed. Table I summarizes all of the orientation relationship information obtained for ζ_m crystals nucleated at grain faces (bounded by grains β_1 and β_2) and grain edges (formed by β_1, β_2 and β_3).

(6) Amongst grain edge-nucleated ζ_m crystals, an exact Burgers orientation was observed with one or two β grains in three of four examples.

(7) Irrespective of whether the orientation relationship across β:ζ_m boundaries was of the Burgers type, some other parallelism of reasonably low indices planes and directions in the two lattices, or irrational, planar facets were a prominent feature of β:ζ_m boundary morphology.

O-Lattice theory has been employed in an effort to predict the possible low energy interphase boundary structures and energies from the observed

(a)

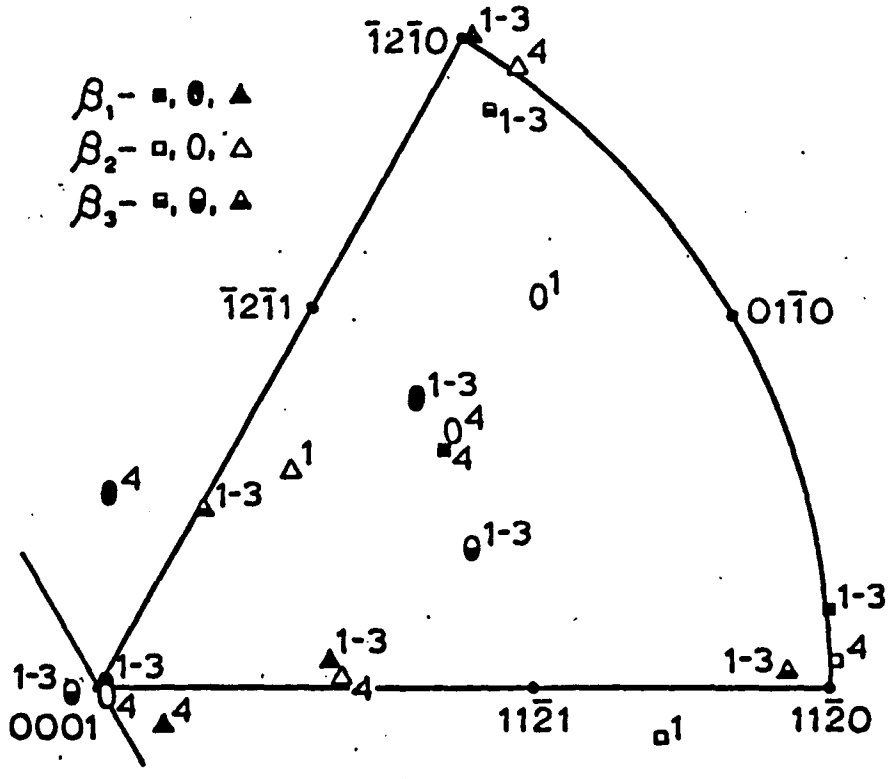

(b)

Figure 1 Orientation relationships between parent β grains and ζ_m crystals in Ag-26a/o Al, (a) 700°C(20 min)→IBQ, and (b) the (0001) stereographic projection of ζ_m crystals showing orientations of the parent β grains relative to $(000\bar{1})_{\zeta_m}$. Superscripts designate the ζ_m crystals with respect to which the various β orientations apply.

Table I

Orientation Relationship Data

Figure No.	Crystal No.	β_1 Grain	β_2 Grain	β_3 Grain
2	1→6	none	$(0001)//(10\bar{1}),[\bar{1}2\bar{1}0]//[\bar{1}\bar{1}\bar{1}]$	-
	7,8	$(0001)//(101),[\bar{1}2\bar{1}0]//[\bar{1}11]$	$(\bar{1}100)//(\bar{1}30),[\bar{1}\bar{1}23]//[\bar{3}\bar{1}1]$	-
3	1→3	none	$(0001)//(10\bar{1}),[11\bar{2}0]//[1\bar{1}\bar{1}]$	-
4	1→4	$(0001)//(\bar{1}\bar{1}0),[11\bar{2}0]//[1\bar{1}\bar{1}]$	$(01\bar{1}0)//(1\bar{2}\bar{1}),[0001]//[\bar{1}0\bar{1}]$	-
5	1→4	$(0001)//(110),[11\bar{2}0]//[\bar{1}11]$	none	-
6	1→6	$(0001)//(101),[11\bar{2}0]//[11\bar{1}]$	$(\bar{1}011)//(\bar{1}01),[2\bar{1}\bar{1}3]//[1\bar{1}1]$	-
7	1→3	$(0001)//(101),[11\bar{2}0]//[\bar{1}11]$	none	-
8	1→3	$(0001)//(011),[\bar{1}2\bar{1}0]//[\bar{1}\bar{1}1]$	none	-
9	1,2	$(0001)//(\bar{1}10),[11\bar{2}0]//[111]$	$(01\bar{1}0)//(112),[4\bar{2}\bar{2}\bar{3}]//[\bar{1}\bar{1}1]$	-
	3	$(1\bar{1}00)//(100),[11\bar{2}3]//[010]$	$(0001)//(01\bar{1}),[11\bar{2}0]//[111]$	
	4	none	$(0001)//(\bar{1}10),[\bar{1}2\bar{1}0]//[11\bar{1}]$	-
10	1→3	$(0001)//(011),[11\bar{2}0]//[\bar{1}\bar{1}1]$	$(1\bar{2}13)//(111),[\bar{1}101]//[\bar{1}\bar{1}2]$	$(0\bar{1}11)/(110),[\bar{1}101]//[001]$
	4	none	$(0001)//(011),[01\bar{1}0]//[0\bar{1}1]$	-
11	1	$(0001)//(101),[01\bar{1}0]//[010]$	$(0001)//(\bar{1}\bar{1}0),[11\bar{2}0]//[1\bar{1}1]$	none
12	1	$(0001)//(110),(2\bar{1}\bar{1}0)//[1\bar{1}1]$	$(0001)//(\bar{1}01),[2\bar{1}\bar{1}0]//[1\bar{1}1]$	none
13	1	none	none	-
	2	none	$(0001)//(011),[01\bar{1}0]//[0\bar{1}1]$	none
14	1	$(0001)//(011),[2\bar{1}\bar{1}0]//[\bar{1}\bar{1}1]$	$(\bar{1}2\bar{1}0)//(10\bar{3}),[10\bar{1}0]//[3\bar{1}\bar{1}]$	-
15	1	$(0001)//(01\bar{1}),[11\bar{2}0]//[111]$	none	-
	2	none	$(0001)//(01\bar{1}),[\bar{1}2\bar{1}0]//[1\bar{1}\bar{1}]$	-
	3	$(0001)//(\bar{1}10),[\bar{1}2\bar{1}0]//[11\bar{1}]$	none	-

orientation relationships between ζ_m and β crystals and thereby explain why the Burgers orientation relationship is so clearly predominant and also determine whether or not at least the conjugate habit plane pairs corresponding to the non-Burgers orientation relationships can be validly described as partially coherent interphase boundaries. The principles and various applications of the O-lattice theory have already been well presented (8,9) and will therefore not be discussed here. The procedure outlined by Bollmann and Nissen (10) was used to calculate the relative boundary energies of various interfaces. It is assumed that a partially coherent $\beta:\zeta_m$ boundary includes two sets, i and j, of parallel misfit-compensating dislocations. An indication of the relative energy of the interface is obtained by calculating the parameter P_{ij}, which is defined as:

$$P_{ij} = \left(\frac{b_i}{d_i}\right)^2 + \left(\frac{b_j}{d_j}\right)^2 \qquad [1]$$

where b is the magnitude of the dislocation Burgers vector, i.e. an estimate of the dislocation line energy, and d is the spacing between the dislocations. From O-lattice theory it is shown that (8,9):

$$(\underline{\underline{I}} - \underline{\underline{A}}^{-1})\underline{x}^{(0)} = \underline{b}^{(L)}$$

where $\underline{\underline{A}}$ is a linear homogeneous transformation relating crystal 1 and crystal 2 and is composed of a rotation, a shear, an expansion, or some combination thereof, $\underline{x}^{(0)}$ is the O-lattice vector and $\underline{b}^{(L)}$ is a difference vector which in the present context corresponds to the Burgers vector of a set of misfit dislocations. Eq. [2] can be inverted if $\mathrm{Det}|\underline{\underline{I}}-\underline{\underline{A}}^{-1}| \neq 0$ to give the O-lattice vectors:

$$\underline{x}^{(0)} = (\underline{\underline{I}} - \underline{\underline{A}}^{-1})^{-1}\underline{b}^{(L)} \qquad [3]$$

The assumption was made that the difference vectors, $b^{(L)}$, used in Eq. [3] are two amongst the ten possible perfect dislocations (not including their negatives) available in the ζ_m crystal structure (11). These dislocations and their magnitudes are presented in Table II. For ease of calculation we have normalized the dislocation line energies by dividing by a. For each dislocation there is a corresponding 0-lattice vector, $\underline{x}^{(0)}$, and each pair of 0-lattice vectors defines an interface. Therefore, taking the dislocations two at a time, a total of 45 interfaces is obtained. The P_{ij} parameter was calculated for each interface. Additionally, P_{ij} was computed at intervals for small rotations of one lattice with respect to the other away from the observed orientation relationships.

1. Exact Burgers Orientation

An attempt was first made to ascertain why the Burgers orientation relationship between β and ζ_m is so clearly predominant. The P_{ij} values for all 45 interfaces constructed from pairs of the perfect dislocations in the h.c.p. lattice listed in Table II are given in Table III. P_{34} is seen to have the lowest value. The dislocations corresponding to this P_{ij}, $1/3\langle 1\bar{2}10\rangle$ and $\langle 0001\rangle$, define the h.c.p. portion of the h.c.p.:b.c.c. interface directly described by the Burgers lattice orientation relationship. Hence the Burgers relationship appears to follow directly from minimization of the interphase boundary energy, as proposed by Bollmann and Nissen (10). Considered further, though, a slightly more subtle argument is required. An orientation relationship is normally established during nucleation rather than during growth. Because of the very small size of a critical nucleus, interfaces which are partially coherent during the later stages of growth are likely fully coherent during nucleation. However, the smaller the P_{ij} value of an interface the less the strain energy required to achieve

Table II. Perfect Dislocations and Their Normalized Line Energies in ζ_{III}

No.	Burgers Vector	Magnitude, $\|b\|$	Normalized Line Energy, $\|b\|/a$
1	$1/3\langle 11\bar{2}0\rangle$	a	1.0
2	$1/3\langle \bar{2}110\rangle$	a	1.0
3	$1/3\langle 1\bar{2}10\rangle$	a	1.0
4	$\langle 0001\rangle$	c	1.627
5	$1/3\langle 11\bar{2}3\rangle$	$\sqrt{c^2+a^2}$	1.910
6	$1/3\langle 1\bar{2}13\rangle$	$\sqrt{c^2+a^2}$	1.910
7	$1/3\langle \bar{2}113\rangle$	$\sqrt{c^2+a^2}$	1.910
8	$1/3\langle 11\bar{2}\bar{3}\rangle$	$\sqrt{c^2+a^2}$	1.910
9	$1/3\langle 1\bar{2}1\bar{3}\rangle$	$\sqrt{c^2+a^2}$	1.910
10	$1/3\langle \bar{2}11\bar{3}\rangle$	$\sqrt{c^2+a^2}$	1.910

Table III. Calculated Values of P_{ij} at the Exact Burgers Orientation

i	j	P_{ij}	i	j	P_{ij}
1	2	2.53×10^{-3}	3	10	2.86×10^{-7}
1	3	6.00×10^{-3}	4	5	8.25×10^{-6}
1	4	1.33×10^{-6}	4	6	1.66×10^{-6}
1	5	1.34×10^{-6}	4	7	5.36×10^{-6}
1	6	1.36×10^{-6}	4	8	8.25×10^{-6}
1	7	1.34×10^{-6}	4	9	1.66×10^{-6}
1	8	1.34×10^{-6}	4	10	5.36×10^{-6}
1	9	1.36×10^{-6}	5	6	9.22×10^{-7}
1	10	1.34×10^{-6}	5	7	1.62×10^{-4}
2	3	6.54×10^{-3}	5	8	2.40×10^{-6}
2	4	8.66×10^{-7}	5	9	6.29×10^{-6}
2	5	8.77×10^{-7}	5	10	1.91×10^{-6}
2	6	8.93×10^{-7}	6	7	8.00×10^{-7}
2	7	8.79×10^{-7}	6	8	6.29×10^{-6}
2	8	8.77×10^{-7}	6	9	4.87×10^{-7}
2	9	8.93×10^{-7}	6	10	9.70×10^{-6}
2	10	8.79×10^{-7}	7	8	1.91×10^{-6}
3	4	2.77×10^{-7}	7	9	9.70×10^{-6}
3	5	2.85×10^{-7}	7	10	1.56×10^{-6}
3	6	2.90×10^{-7}	8	9	9.22×10^{-7}
3	7	2.86×10^{-7}	8	10	1.62×10^{-4}
3	8	2.85×10^{-7}	9	10	8.00×10^{-7}
3	9	2.90×10^{-7}			

full coherency. Although the structural component of interphase boundary energy is zero for all fully coherent interfaces, the less the strain energy needed to achieve full coherency the smaller will be the depression of the coherent solvus for a particular interface relative to the incoherent solvus, and hence at a given reaction temperature the higher will be the volume free energy change driving nucleation. On Gibbsian nucleation theory, even small differences in this driving force result in enormous differences in the nucleation rate. Hence the critical nucleus shape made up from interfaces for which the driving force is largest is by far the most likely one to form.*

2. Other Rational-Type Orientation Relationships

Table I shows that 11 non-Burgers orientation relationships describable in terms of parallel planes and directions with reasonably low indices were experimentally observed. In order to ascertain whether or not each of them corresponds to a partially coherent interface containing two sets of parallel misfit dislocations not too closely spaced, the 45 possible interfaces were computed for each one, together with the associated P_{ij}. Small orthogonal rotations about the observed orientation relationships were essayed in attempts to seek still lower P_{ij} values. The results obtained for the interfaces with the lowest P_{ij}'s are summarized in Table IV. Even the smallest interdislocation spacing, 2.69 nm, is 80% larger than the smallest such spacing so far observed with TEM (12). Most of the other spacings fall comfortably within the range of more commonly observed spacings (13,14). Hence these interfaces may be considered to be valid partially coherent boundaries.

*The assumption is thus made that the chemical interfacial energy is the same for all coherent interfaces considered.

Table IV. Possible Partially Coherent Interfaces for the Observed Non-Burgers Orientations

Fig. No.	Crystal No.	Orientation Relationships	Angle (b_i, b_j)	b_i	d_i (nm)	b_j	d_j (nm)	P_{ij}	Rotation Away From Observed Orientation ~Axis	Angle
2	7,8	$(\bar{1}\bar{1}00)//(\bar{1}\bar{3}0)$ $[\bar{1}\bar{1}23]//[\bar{3}\bar{1}\bar{1}]$	20.5°	$\frac{1}{3}\langle 11\bar{2}0\rangle$	3.61	$\frac{1}{3}\langle\bar{2}110\rangle$	4.56	$P_{12}=1.25\times10^{-3}$	[75 $\bar{7}\bar{8}$ 3 15]	2.3°
4	1↔4	$(01\bar{1}0)//(1\bar{2}\bar{1}\bar{1})$ $[0001]//[\bar{1}0\bar{1}]$	21.1°	$\frac{1}{3}\langle 1\bar{2}10\rangle$	8.85	$\frac{1}{3}\langle 1\bar{2}1\bar{3}\rangle$	5.71	$P_{39}=1.25\times10^{-3}$	[$\bar{1}$ 2 $\bar{1}$ 13]	5.6°
6	1↔6	$(\bar{1}011)//(\bar{1}01)$ $[2\bar{1}\bar{1}3]//[1\bar{1}1]$	55.0°	$\frac{1}{3}\langle\bar{2}110\rangle$	4.23	$\frac{1}{3}\langle 1\bar{2}1\bar{3}\rangle$	19.6	$P_{29}=6.55\times10^{-4}$	[$\bar{3}$ $\bar{6}$ 9 10]	1.7°
9	1,2	$(01\bar{1}0)//(112)$ $[4\bar{2}\bar{2}3]//[\bar{1}\bar{1}1]$	36.5°	$\frac{1}{3}\langle 1\bar{2}10\rangle$	3.66	$\frac{1}{3}\langle\bar{2}11\bar{3}\rangle$	9.21	$P_{310}=1.17\times10^{-3}$	$[01\bar{1}0]$	1.0°
	3	$(1\bar{1}00)//(100)$ $[11\bar{2}\bar{3}]//[010]$	--	--	--	--	--	none	--	--
10	1(β_2)	$(1\bar{2}13)//(111)$ $[\bar{1}101]//[\bar{1}\bar{1}2]$	--	--	--	--	--	none	--	--
	1↔3(β_3)	$(0\bar{1}11)//(110)$ $[\bar{1}101]//[001]$	23.4°	$\frac{1}{3}\langle\bar{2}110\rangle$	6.85	$\frac{1}{3}\langle\bar{2}113\rangle$	112	$P_{27}=1.63\times10^{-4}$	none	0.0°
	4	$(00\acute{0}1)//(011)$ $[01\bar{1}0]//[0\bar{1}1]$	55.9°	$\frac{1}{3}\langle 11\bar{2}0\rangle$	14.2	$\frac{1}{3}\langle 1\bar{2}10\rangle$	7.25	$P_{13}=2.40\times10^{-3}$	$[12\bar{3}0]$	1.6°
11	1	$(0001)//(101)$ $[01\bar{1}0]//[010]$	90.0°	$\frac{1}{3}\langle\bar{2}110\rangle$	2.62	$\langle 0001\rangle$	1260	$P_{24}=1.38\times10^{-3}$	[0001]	2.0°
13	2	$(0001)//(011)$ $[01\bar{1}0]//[0\bar{1}1]$	55.9°	$\frac{1}{3}\langle 11\bar{2}0\rangle$	14.2	$\frac{1}{3}\langle 1\bar{2}10\rangle$	7.25	$P_{13}=2.40\times10^{-3}$	$[12\bar{3}0]$	1.6°
14	1	$(\bar{1}2\bar{1}0)//(10\bar{3})$ $[10\bar{1}0]//[3\bar{1}1]$	--	--	--	--	--	none	--	--

Interfacial energy may also serve as a means for distinguishing between partially coherent and disordered or incoherent interphase boundaries. This criterion was utilized in very approximate fashion by noting that calculations show that P_{34} approaches 10^{-2} at a 5° rotation about $[\bar{1}100]_{\zeta_m}$. This value was taken to be appropriate for a disordered boundary; hence only interfaces with a P_{ij} below this level were taken to fall in the partially coherent category.

Note in Table IV that for three of the orientation relationships experimentally observed a corresponding partially coherent interphase boundary could not be identified. The micrographs of the ζ_m crystals involved, however, indicated that pronouncedly linear facets were present on these crystals. Also in the five cases in which ζ_m crystals appeared to have no reasonably low indices orientation relationship with respect to a β grain they exhibited pronounced facets at the boundary with this grain. At least in precipitation reactions, faceting during growth has been found to be a good indication of the presence of a barrier to growth in the form of a partially or fully coherent interface (13-15). Failure to identify partially coherent boundaries with the experimental and theoretical techniques employed in the present investigation, however, does not constitute complete proof that the facets do not have such a structure. The conjugate habit planes forming the facets were not identified. If these planes are different from those specified by the orientation relationships but are derivable from these relationships they could still have a partially coherent structure.

An alternate explanation for the two sets of results which are inconsistent with faceted ζ_m morphologies derives from nucleation theory.

Particularly since the ζ_m crystals nucleated at grain faces or edges, the kinetic advantage achieved (through minimization of the activation free energy for nucleation) by a lattice orientation relationship which permits low energy $\beta:\zeta_m$ boundaries to be formed with respect to both or all three β grains could well result in compromise orientation relationships (16) under some circumstances of grain boundary crystallography. Deviations of nearly 10° from an orientation relationship which does permit two-dislocation interphase boundaries to develop could be accomodated through the introduction of one or more additional sets of dislocations, orthogonal to the plane of the first two sets. A mathematical search for more "hospitable" nearby orientation relationship, however, would be as tedious as it would be unconvincing. High-resolution TEM studies of interfacial structure are required to fill this lacuna. A prolonged attempt to make such an investigation in the present alloy was unfortunately defeated by thin foil preparation problems. Another study of this type, however, is presently in progress in a more amenable alloy system (17).

3. Re-examination of Available Experimental Evidence on Orientation Relationships

There is much experimental evidence in the literature which bears on the results of the present investigation. A careful review has been made of all the quantitative data on orientation relationships and habit planes which could be located for massive transformations (6,18-21). We conclude, Massalski (22) to the contrary, that none of this evidence unambiguously conflicts with the results of the present investigation.

An opportunity to debate this and other central issues concerning the mechanism of the massive transformation will arise during a one-session symposium on this transformation to be held during the Fall, 1980 TMS-MSD Meeting under the sponsorship of the Phase Transformations Technical

Activity of the Materials Science Division, ASM. This symposium has been organized by M. R. Plichta and H. I. Aaronson. Participants will include Prof. Mats Hillert (Royal Institute of Technology, Sweden), discussing the thermodynamics of the massive transformation, Prof. T. B. Massalski (Carnegie-Mellon University), considering the internal structure associated with the transformation, Prof. J. H. Perepezko (University of Wisconsin, Madison), discussing the evidence on growth kinetics (Profs. Massalski and Perepezko will co-author each others' talks and papers) and M. R. Plichta, W. A. T. Clark and H. I. Aaronson presenting their views on the nucleation and crystallography of this transformation. The proceedings of this symposium will be published in Metallurgical Transactions under the editorship of M.R.P. and H.I.A.

B. Nucleation Kinetics of the $\beta \rightarrow \alpha_m$ Transformation in Ti-Ag and Ti-Au
(M. R. Plichta, Graduate Student)

Nearly all of the work undertaken on this project has been previously reported to AFOSR. In this sub-section we summarize a recent supplement to this project. This supplement follows directly from work done at the end of the recently completed Ph.D. thesis of W. F. Lange III (23) on the nucleation kinetics of proeutectoid ferrite at austenite grain boundaries. It may be recalled that the model of the critical nucleus originally used by Lange, and directly adapted to present purposes, is that of Figure 2a. In this model not only the edges but also both the upper and lower broad faces of the pillbox were taken to be coherent and to lie in energy cusp orientations. Lange subsequently recognized that if the energy of one of the pillbox broad faces was assumed to be sufficiently (but still reasonably) low, the other would have an energy high enough to be disordered, and hence to have the equilibrium shape

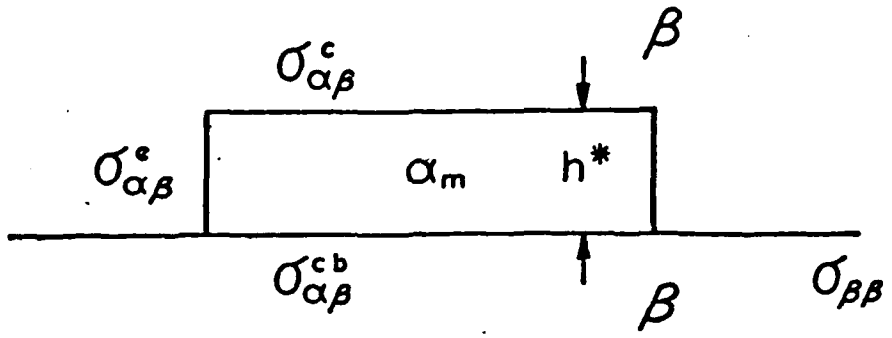

(a)

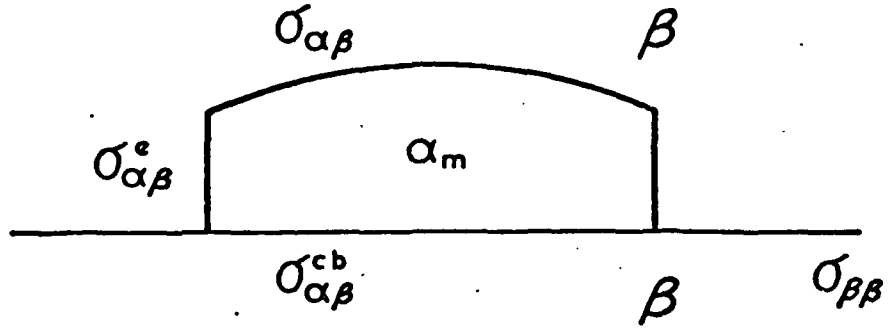

(b)

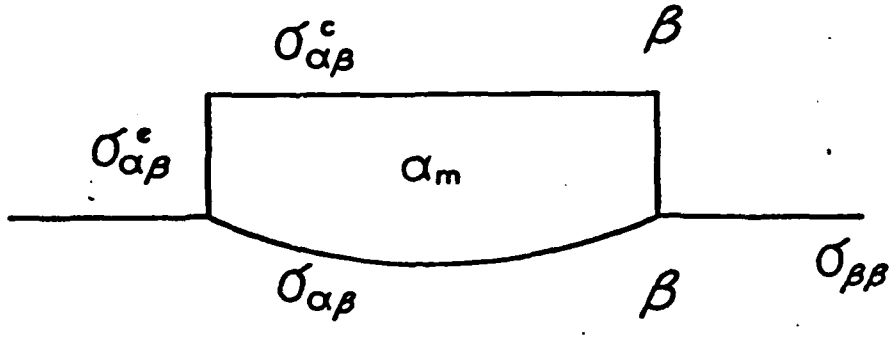

(c)

Figure 2 - Variants on the pillbox-type critical nucleus shape. Lange (23).

of a spherical cap. The two possible variations in critical nucleus morphology thereby allowed are shown as Figures 2b and 2c. Lange has shown that both variations lead to the same nucleation rate equation, but one which is somewhat different than that for the model of Figure 1a:

$$J^* = \frac{2Dx_\beta v_\alpha \varepsilon'}{a^6 (3kTA\sigma_{\alpha\beta})^{1/2}} \exp\left[\frac{-(4\pi(\sigma^e_{\alpha\beta})^2\varepsilon' + \frac{16\pi\sigma^3_{\alpha\beta} f(\psi)}{3}}{\phi^2 kT}\right]$$

where, $$\varepsilon' = \sigma^{c(b)}_{\alpha\beta} + \sigma_{\alpha\beta}\cos\psi - \sigma_{\beta\beta}$$

$$A = \left(\frac{\varepsilon' \sin^2\psi}{\sigma_{\alpha\beta}} + \frac{4}{3} f(\psi)\right)$$

$$f(\psi) = \frac{(2 - 3\cos\psi + \cos^3\psi)}{4}$$

$$\sin\psi = \frac{\sigma^e_{\alpha\beta}}{\sigma_{\alpha\beta}}$$

where J^* = no. of nuclei/un. grain boundary area/un. time, x_β = atom fraction of solute in the matrix, v_α = average volume/atom in the nucleus, $a \cong$ one lattice parameter, k = Boltzmann's constant, T = absolute temperature, $\sigma_{\alpha\beta}$ = interfacial energy of a disordered α:β boundary, ϕ = sum of the volume free energy change and the volume strain energy attending nucleation, $\psi = \sin^{-1} \sigma_{\alpha\beta}/\sigma_{\beta\beta}$, $\sigma^e_{\alpha\beta}$ = interfacial energy of the pillbox edges, $\sigma_{\beta\beta}$ = grain boundary energy and $\sigma^{c(b)}_{\alpha\beta}$ = interfacial energy of a coherent α:β boundary which is coplanar with the grain boundary.

Using this nucleation rate equation, the experimentally measured nucleation rates, reasonable estimates of $\sigma_{\alpha\beta}$ and $\sigma_{\beta\beta}$ and other ancillary data as indicated, $\sigma^e_{\alpha\beta}$ can be obtained by an iterative process. The results

are given in Table V together with the previously reported results for the coherent pillbox of Figure 2a. We see that the calculated edge energies range from 17 ergs/cm^2 at the lower undercoolings to 60 ergs/cm^2 at the higher undercoolings. These values, though slightly lower than those obtained from the coherent pillbox, are again about as expected for a coherent interphase boundary in titanium alloys. Hence the models of Figures 2b and 2c are also consistent with the nucleation rate data. In the context of the orientation relationship results obtained on the $\beta \rightarrow \zeta_m$ transformation in Ag-26 A/O Al, which we feel ought to be applicable in essence to the $\beta \rightarrow \alpha_m$ transformation in Ti-Ag and Ti-Au, however, the models of Figures 2b and 2c may be more realistic in a significant number of cases, particularly if TEM studies eventually show that facets do not always correspond to partially or fully coherent interphase boundaries. Hence it is comforting to find that a pillbox coherent at the matrix grain boundary is not required, on Gibbsian nucleation theory, to account for such crystallographic observations.

C. The f.c.c. $\alpha \rightarrow$h.c.p. α_2 Massive Transformation in Au-Cd
(J. P. Moore, Graduate Student)

This program is being undertaken in order to secure the most definitive possible evidence that specific, reproducible, low energy orientation relationships obtain between the product of a massive transformation and its matrix phase. Matching between the f.c.c. and the h.c.p. lattices is the best that can possibly be secured between two common, distinctly different crystal structures. Hence plate shaped precipitates formed during the usual precipitation from solid solution reaction tend to have exceptional perfection and very high length/width ratios when the matrix is f.c.c. and the precipitate is h.c.p., or vice versa (24,25). Following the dictum of Massalski (22), we sought a f.c.c.$\rightarrow$h.c.p. massive transformation in a system where both

Table V. Calculated Nucleus Edge Energy vs. Nucleus Height

Alloy	Temperature (°K)	Pillbox Height (atomic distances)	Figure 4a		Figure 4b and 4c		
			$\sigma^{e}_{\alpha\beta_2}$ (mJ/m^2)	Incubation Time (μsec)	$\sigma^{e}_{\alpha\beta_2}$ (mJ/m^2)	$\sigma^{c}_{\alpha\beta}$ ($\sigma^{cb}_{\alpha\beta}$) (mJ/m^2)	Incubation Time (μsec)
Ag I	1116	2	34.7	1.4	32.3	177.4	0.07
		4	24.6	1.0	24.6	178.8	0.04
	1073	2	57.3	0.33	53.5	182.0	0.03
		4	40.7	0.23	40.6	186.0	0.01
Ag II	1105	2	33.1	1.2	30.9	177.2	0.06
		4	23.5	0.84	23.5	178.5	0.03
	1048	2	59.7	0.23	55.9	182.7	0.02
		4	42.4	0.16	42.4	187.3	0.01
Ag III	1101	2	23.2	2.6	21.7	176.1	0.09
		4	16.5	1.8	16.5	176.7	0.05
	1050	2	51.3	0.27	48.0	180.7	0.02
		4	36.4	0.19	36.4	184.0	0.01
Au I	1094	2	29.9	4.1	27.9	176.8	0.19
		4	21.2	2.9	21.3	177.9	0.09
	1058	2	50.2	0.87	47.2	180.6	0.07
		4	36.7	0.62	35.8	183.9	0.03

phases would be disordered, substitutional solid solutions. Many other requirements were imposed, such as a well established phase diagram, the availability of thermodynamic data, reasonable transformation temperatures, etc.; after a thorough search through available compilations of phase diagrams, the Au-Cd system was selected. Figure 2 shows the Au-rich portion of this phase diagram. The three arrowheads indicate the alloy compositions we plan to prepare in this system. Note that the temperature range of the $\alpha + \alpha_2$ region is usually limited and that the T_o temperature (which approximately bisects this region) extends over an exceptionally wide range, of ca. 200°C. The former implies limited competition from precipitation of equilibrium α_2 while the latter raises the possibility of exploring a substantial transformation temperature regime despite the notorious rapidity of massive transformation kinetics.

A small volume of an exploratory alloy containing 30 A/O Cd was prepared from 99.99% pure materials, melted in Vycor under a helium atmosphere and then quenched. The ingot was then re-encapsulated and homogenized for 48 hrs. at 625°C. Specimens 1×10^{-2} m. x 5×10^{-3} m. x 3×10^{-4} m. were cut from the ingot, solution annealed at 625°C for 5 min. and quenched into iced brine. They were then electropolished with a HCl-25% ethanol-25% glycerol solution at room temperature, at 3.7 volts D.C. Much difficulty has been encountered with electropolishing technique; improvements are still being made; however, as Figure 3 shows (this was taken with an SEM at 500X), usable results have been obtained. This micrograph shows a dramatically plate-filled microstructure, with no more than a trace of grain boundary allotriomorphs along a few grain boundaries in the α matrix. This structure bears no resemblance at all to the usual massive transformation product, but is precisely what we had hoped to find. Also quite appealingly, despite

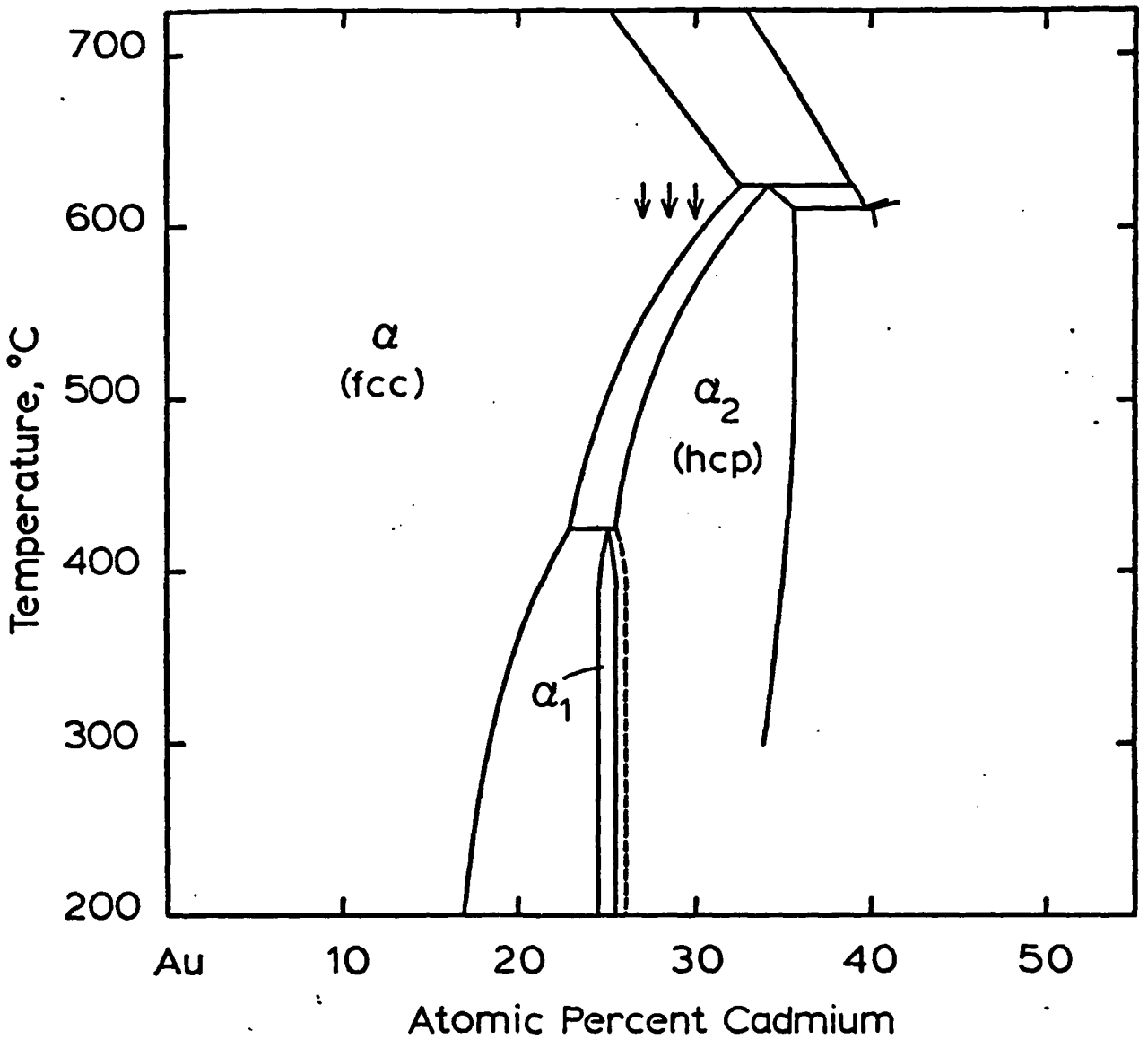

Figure 3 - Au-rich portion of Au-Cd phase diagram. Hansen (27).

the fact that this is the most Cd-rich alloy planned, and hence has the highest T_o temperature, transformation kinetics are not exceedingly rapid—presumably as a result of the crystallographic barrier to growth at the broad faces of the α_2 plates.

With much assistance from Dr. G. K. Scarr, a preliminary survey has been made of the transmission electron microscopic structure of specimens quenched from the α region into iced brine to yield an $\alpha + \alpha_2$ microstructure.

Thin foils were prepared by ion milling, specimens ca. 50 μm thick being bombarded by 6.5 kV Ar ions for 6 hrs. Results obtained were usable, but not adequate for quantitative work. Artifacts appear to have been introduced during the ion bombardment; use of our cold stage ("miller chiller") may permit them to be eliminated. (A cyanide solution is also being tried for thin foil preparation, but to date the results have been erratic.) Selected area electron diffraction was used to confirm the identity of h.c.p. massive α_2 and of retained f.c.c. α. Stacking faults were observed in both phases. They often occur in large numbers. But there is no indication that α_2 is formed by the Nicholson-Nutting (26) stacking fault dissociation mechanism, which would greatly complicate the microstructure developed. And the density of faults seems usually insufficient in either phase to interfere with interfacial structure determinations by means of high-resolution TEM.

Accordingly, we have accepted the $\alpha \rightarrow \alpha_2$ Au-Cd transformation as our prototype f.c.c.→h.c.p. massive transformation and have ordered a supply of high-purity Au and Cd which should be sufficient for the purposes of Mr. Moore's Ph.D. thesis.

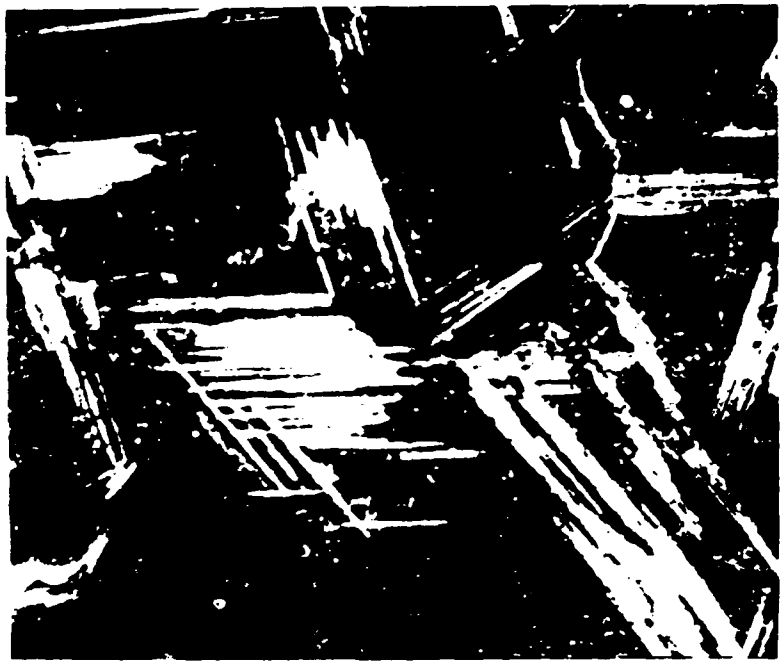

Figure 4 - SEM photograph of α_2 plates (light) in retained α (dark) matrix. Au-30 A/O Cd. X500.

References

1. H. I. Aaronson: The Mechanism of Phase Transformations in Crystalline Solids, p. 270, Inst. of Metals, London (1969).

2. C. G. Rhodes and J. C. Williams: Met. Trans., 6A, 1670 (1975).

3. C. G. Rhodes and J. C. Williams: ibid, 6A, 2103 (1975).

4. W. G. Burgers: Physica, 's Grav., 1, 561 (1934).

5. D. J. H. Cockayne: Jnl. of Microscopy, 98, (2), 116 (1973).

6. J. D. Ayers and D. C. Joy: Acta Met., 20, 1371 (1972).

7. H. B. Aaron and H. I. Aaronson: Met. Trans., 2, 23 (1971).

8. W. Bollmann: Phil. Mag., 16, 383 (1967).

9. W. Bollmann: Crystal Defects and Crystalline Interfaces, Springer-Verlag, Berlin (1970).

10. W. Bollmann and H.-U. Nissen: Acta Cryst., A24, 546 (1968).

11. D. Hull: Introduction to Dislocations, p. 122, Pergamon Press, New York (1975).

12. J. M. Rigsbee and H. I. Aaronson: Acta Met., 27, 365 (1979).

13. H. I. Aaronson, C. Laird and K. R. Kinsman: Phase Transformations, p. 313, ASM, Metals Park, OH (1970).

14. H. I. Aaronson: Jnl. of Microscopy, 102, 275 (1974).

15. H. I. Aaronson, J. K. Lee and K. C. Russell: Precipitation Processes in Solids, p. 31, TMS-AIME, New York (1979).

16. M. Hillert: Decomposition of Austenite by Diffusional Processes, p. 197, Interscience Publishers, New York (1962).

17. W. A. T. Clark and H. I. Aaronson: Michigan Technological University, unpublished research (1979).

18. T. B. Massalski: Acta Met., 6, 243 (1958).

19. E. B. Hawbolt and T. B. Massalski: Met. Trans. 1, 2315 (1970).

20. J. Perkins and T. B. Massalski: ibid, 2, 2701 (1971).

21. D. Hull and R. D. Garwood: Mechanism of Phase Transformations in Metals, p. 219, Inst. of Metals, London (1956).

22. T. B. Massalski: Phase Transformations, p. 433, ASM, Metals Park, OH (1970).

23. W. F. Lange III, Ph.D. Thesis, Michigan Technological University (1979).

24. C. Laird and H. I. Aaronson: Acta Met., 15, 73 (1967).

25. K. R. Kinsman, H. I. Aaronson and E. Eichen: Met. Trans., 2, 1041 (1971).

26. R. B. Nicholson and J. Nutting: Acta Met., 9, 332 (1961).

27. M. Hansen: Constitution of Binary Alloys, p. 192, McGraw-Hill, New York (1958).

Cumulative Grant Publications List

1. K. F. Michaels, W. F. Lange III, J. R. Bradley and H. I. Aaronson: "Considerations on the Kaufman Approach to Binary Phase Diagram Calculation", Met. Trans., 1975, vol. 6A, p. 1843.

2. M. R. Plichta, J. M. Rigsbee, M. G. Hall, K. C. Russell and H. I. Aaronson: "Nucleation Kinetics of the Massive Transformation in Cu-Zn in the Presence and Absence of Special Orientation Relationships", Scripta Met., 1976, vol. 10, p. 1065.

3. M. R. Plichta, J. C. Williams and H. I. Aaronson: "On the Existence of the $\beta \rightarrow \alpha_m$ Transformation in the Alloy Systems Ti-Ag, Ti-Au and Ti-Si", Met. Trans. A, 1977, vol. 8A, p. 1885.

4. H. I. Aaronson, M. R. Plichta, G. W. Franti and K. C. Russell: "Precipitation at Interphase Boundaries", Met. Trans., 9A, 363 (1978).

5. B. W. Bennett, G. J. Shiflet and H. I. Aaronson: "Regular Solution Theory Calculation of the Congruent Transformation Point of a Solid Solution", CALPHAD, 2, 209 (1978).

6. M. R. Plichta, H. I. Aaronson and J. H. Perepezko: "Thermodynamics and Kinetics of the $\beta \rightarrow \alpha_m$ Transformation in Three Ti-X Systems", Acta Met., 26, 1293 (1978).

7. T. P. Diebold, H. I. Aaronson and G. W. Franti: "Influence of Interphase Boundary Structure upon the Mechanism of Eutectoid Decomposition in a Ti-Ni Alloy", Met. Trans., 9A, 1339 (1978).

8. G. W. Franti, J. C. Williams and H. I. Aaronson: "A Survey of Eutectoid Decomposition Mechanisms in Ten Ti-X Systems", Met. Trans., 9A, 1641 (1978).

9. H. I. Aaronson: "Mechanisms of Diffusional Growth", Phase Transformations, Vol. 1, p. II-1, The Institution of Metallurgists/Chameleon Press (April, 1979).

10. G. J. Shiflet, J. K. Lee and H. I. Aaronson: "Application of the Kaufman Approach to the Calculation of Intra-Rare Earth Phase Diagrams, CALPHAD, in press.

11. M. R. Plichta, H. I. Aaronson, J. C. Williams and G. W. Franti: "Mechanisms of Precipitation from Massive α in Three Ti-X Systems and the Meyrick Theory of Cellular Reaction Initiation", Scripta Met., 13, 407 (1979).

12. M. R. Plichta, J. H. Perepezko, H. I. Aaronson and W. F. Lange III: "Nucleation Kinetics of Massive α in Ti-Ag and Ti-Au Alloys", ready for submission to Acta Met.

13. M. R. Plichta and H. I. Aaronson: "Crystallography and Morphology of the $\beta \rightarrow \zeta_m$ Transformation in Ag-26 A/O Al", ready for submission to Acta Met.